

# A Comparative Study of Mechanical Alloying and Mechanical Milling of $\text{Nd}_8\text{Fe}_{88}\text{B}_4$

Q. Zeng, Y.F. Xiao, X.B. Liu, S.Z. Dong, Y.S. Deng, Z.Y. Zhang, and R. Wang

(Submitted 6 November 1997; in revised form 23 January 1998)

**A comparative study was made of structure and magnetic properties of  $\text{Nd}_8\text{Fe}_{88}\text{B}_4$  prepared by mechanical alloying (MA) using elemental powders as starting materials and by mechanical milling (MM) of the alloy. X-ray diffraction (XRD) and differential scanning calorimetry (DSC) combined with transmission electron microscopic (TEM) studies revealed that both milling procedures resulted in a mixture of  $\alpha$ -Fe and an amorphous phase. The thermal stability of the as-milled powders produced by MA was comparable to that of the as-milled powders produced by MM. Heat treatment of the milled powders above the crystallization temperature resulted in the formation of a nanocrystalline mixture of  $\text{Nd}_2\text{Fe}_{14}\text{B}$  and  $\alpha$ -Fe, but annealed MA powders demonstrated a somewhat coarser structure in comparison with annealed MM powders. Therefore, higher remanences and coercivities were obtained by MM.**

**Keywords** mechanical alloying, mechanical milling, nanocrystalline materials, Nd-Fe-B alloys, permanent magnets

## 1. Introduction

High energy ball milling was first used to produce oxide dispersion strengthened superalloys and subsequently has been widely used as a unique means of preparing alloy and compounds (Ref 1-3). A distinction between mechanical alloying (MA) and mechanical milling (MM) is that elemental powders are milled in MA, and the already alloyed materials are milled in MM. In the Nd-Fe-B system alloys, amorphous Nd-Fe-B materials have been produced by MM (Ref 4). The defects introduced by the deformation during milling are responsible for raising the free energy of the crystalline materials to that of the amorphous phase (Ref 5). Schultz et al. (Ref 6) showed that the MA of the mixture of pure crystalline components does not result in the formation of either crystalline or amorphous materials; however, Harada et al. (Ref 7) showed that an amorphous phase was formed in the Nd-Fe-B system by MA. Recently it has been demonstrated that amorphization occurs even in some alloys that have a heat of mixing of the amorphous alloy that is higher than that of the mixture of the corresponding pure crystalline components (Ref 8-10). In such cases, the stored energy of cold work accumulated during MA—which consisted of repeating mechanical mixing, cold welding, fracturing, and rewelding powders—might be the driving force for the amorphization.

The magnetic properties of MA materials with lower Nd (11.8 at.%) NdFeB alloys are inferior to those of their rapidly quenched counterparts (Ref 11, 6). In contrast, MM powders exhibit comparable magnetic properties to rapidly quenched alloys (Ref 12).

Recently, nanocomposite permanent magnets showing remanence enhancement have created considerable interest (Ref

12-17); It is believed that the remanence enhancement is associated with exchange coupling between the magnetically hard and soft phases (Ref 17, 16). To enable the exchange coupling to be effective, the grain sizes of the hard and soft phases should be approximately 10 nm.

A comparative study of the microstructure and magnetic properties of MA and MM two-phase  $\text{Nd}_8\text{Fe}_{88}\text{B}_4$  alloys was made, and the results were reported.

## 2. Experimental Details

The elemental powders used for MA were Nd (99.9%, <10  $\mu\text{m}$ ), Fe (99.9% average diameter 5  $\mu\text{m}$ ), B (99.99%, <5  $\mu\text{m}$ ), ingots for MM were prepared by arc melting 99.9% pure Nd, Fe, and B pieces under an argon atmosphere. The ingots were then crushed into powders with particle diameters <0.5 mm. In both cases, a starting composition of  $\text{Nd}_8\text{Fe}_{88}\text{B}_4$  was used. The MA and MM were performed for milling time up to 24 h at a speed of 600 rpm by using a high-energy ball mill with a ball-to-powder weight ratio of 20 to 1. Heat treatment of the as-milled powders was conducted from 550 to 850 °C for 0.5 h under pressures lower than  $10^{-3}$  Pa.

The powders were characterized by XRD using copper  $K\alpha$  radiation at room temperature. Thermal properties of as-milled powders were examined under an argon atmosphere using differential scanning calorimetry (DSC) at a heating rate of 15 k/min. The morphology was investigated under a TEM. After the powders were mixed with epoxy resin and cold pressed into cylinders, the magnetization of the powder was measured using a vibrating sample magnetometer (VSM) with a maximum applied field of 50 k Oe at room temperature. The saturation magnetization was estimated by extrapolation.

## 3. Results and Discussion

A typical XRD pattern of as-milled powder is shown in Fig. 1. The diffraction patterns of the as-milled samples regardless of MM or MA showed only broadened peaks corresponding to the

**Q. Zeng**, Beijing Institute of Aeronautical Materials, Post Box 81-78, Beijing, China, 100095; and **Y.F. Xiao, X.B. Liu, S.Z. Dong, Y.S. Deng, Z.Y. Zhang,** and **R. Wang**, Institute of Materials Science and Engineering, University of Science and Technology Beijing, Beijing China, 100083. Contact e-mail: dr.qizeng@263.net.

$\alpha$ -Fe phase. The TEM selected area diffraction patterns revealed the presence of an amorphous phase in addition to  $\alpha$ -Fe. According to the equilibrium phase diagram, the  $\text{Nd}_8\text{Fe}_{88}\text{B}_4$  alloy pertains to a two-phase region ( $\text{Nd}_2\text{Fe}_{14}\text{B} + \alpha\text{-Fe}$ ) (Ref 18). From the thermodynamic point of view, crystalline  $\text{Nd}_8\text{Fe}_{88}\text{B}_4$  has a lower free energy than the elemental powder mixtures and the amorphous phase. For MM, the defects introduced by the deformation and large surface energy due to micrometer grain size during milling is responsible for raising the free energy of the crystalline materials to that of the amorphous phase. For MA, amorphous phase suggests that the high energy accumulated by ball milling during MA contributes to the amorphization. The estimated temperature rise during the MA due to the impact of the milling media is estimated as  $<300$  K (Ref 19), so that diffusion of the atoms to form the intermetallic  $\text{Nd}_2\text{Fe}_{14}\text{B}$  compounds seems to be quite limited.

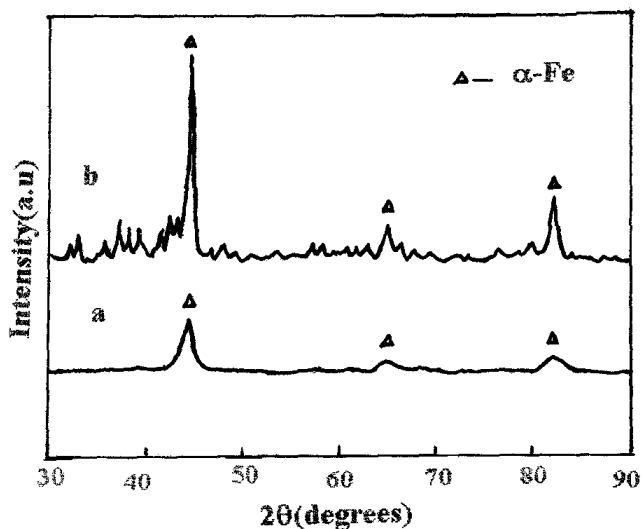


Fig. 1 X-ray diffraction of  $\text{Nd}_8\text{Fe}_{88}\text{B}_4$ , (a) as-milled and (b) annealed at 873 K for 0.5 h

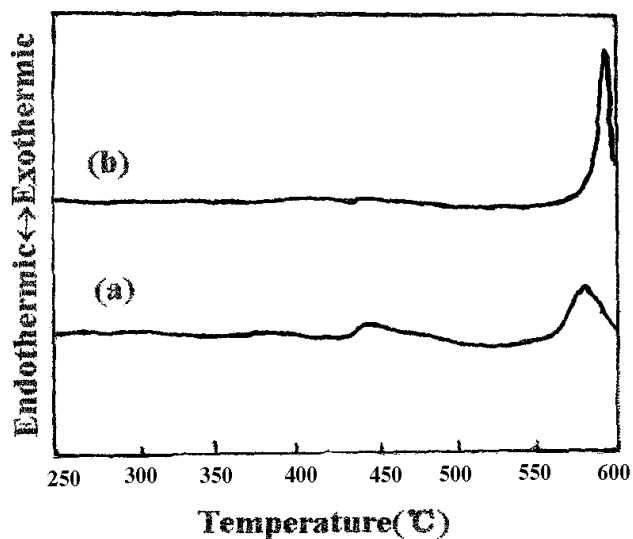


Fig. 2 Differential scanning calorimetry curves of (a) as-milled MA and (b) as-milled MM powders taken at a heating rate of 0.33 K/s

A typical diffraction pattern of an annealed sample is also shown in Fig. 1. The diffraction patterns of the MM and MA powders were similar. Heat treatment at or above 823 K for 0.5 h resulted in the crystallization of the magnetically hard  $\text{Nd}_2\text{Fe}_{14}\text{B}$  phase. The resulting structure consisted of a mixture of  $\text{Nd}_2\text{Fe}_{14}\text{B}$  and  $\alpha\text{-Fe}$ . The result suggests that the powders produced by MA are of a similar nature as the powders obtained from MM. This also suggests that the temperature during MM and MA had been kept lower than the crystallization temperature of the amorphous phase.

Figure 2 shows the DSC curves of as-milled MM and MA powders. The DSC curve of the MA powder showed two exothermic peaks at  $\sim 450$  and  $\sim 570$  °C. The low temperature peak may be attributed to recrystallization and/or grain growth of the  $\alpha\text{-Fe}$  phase (Ref 20, 21), and the second exothermic peak at 845 K is due to a crystallization reaction in contrast to the MA sample, the DSC curve for the MM sample showed only one exothermic peak at approximately 860 K, higher than the peak value of MA.

Figure 3 shows the dark-field TEM micrographs of MM and MA samples annealed at 873 K for 0.5 h. Energy disperse spectroscopy analysis with a probe size of 15 nm failed to

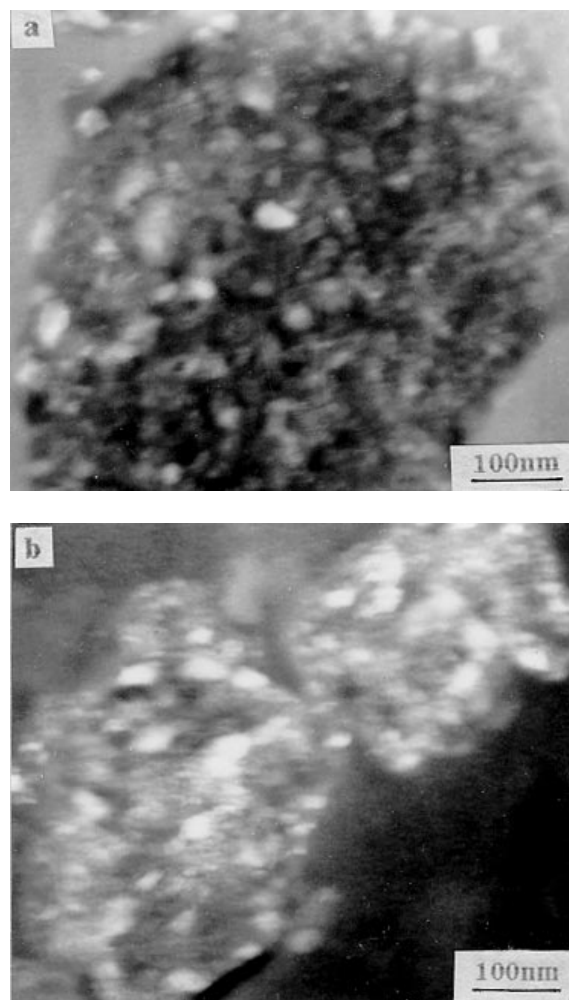


Fig. 3 Dark-field TEM micrographs of (a) MA and (b) MM powders annealed at 873 K for 0.5 h

distinguish between grains of 2:14:1 phase and  $\alpha$ -Fe. The MM sample consists of a homogeneous mixture of 2:14:1 phase and  $\alpha$ -Fe with an average grain size of approximately 20 to 30 nm, the MA sample also shows a homogeneous mixture of the two phases, but the grains are larger (approximately 30 to 50 nm) in diameter. The grain size of both the MA and MM powders increased with increasing annealing temperature. However, the average grain size of MA powder was always larger than that of MM powders.

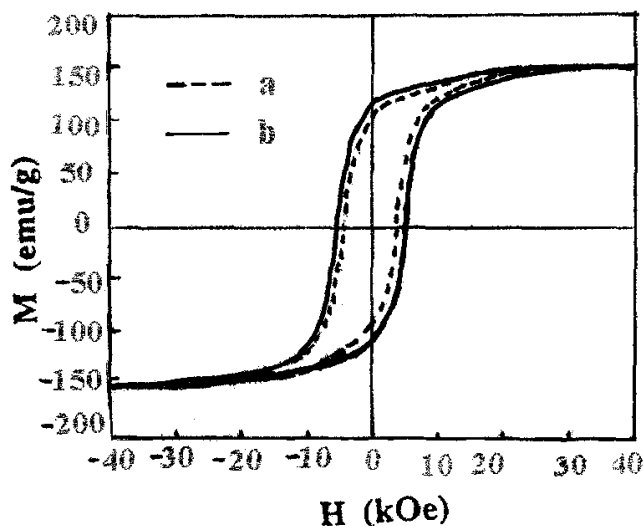


Fig. 4 Hysteresis loop of (a) MA and (b) MM powders annealed at 873 K for 0.5 h

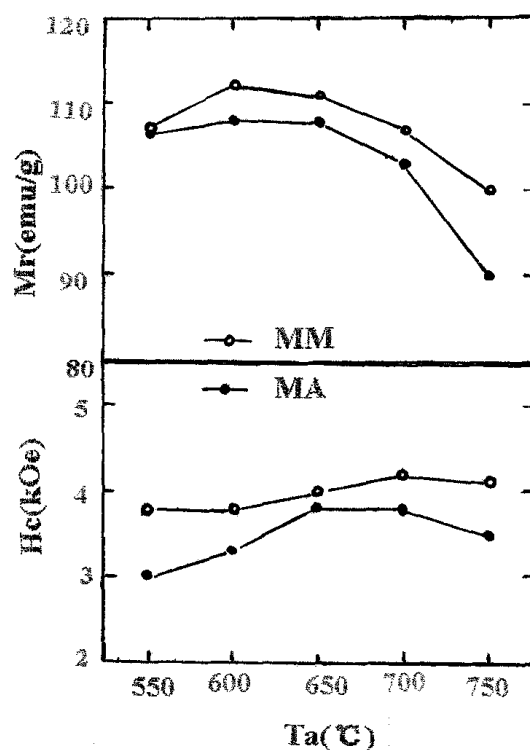


Fig. 5 Variation of  $M_r$  and  $H_c$  of MM and MA powder with annealing temperature

The saturation magnetization ( $M_s$ ) of the as-milling MM powder is 151 emu/g, while  $M_s$  of the MA powder is 164 emu/g. The difference may be due to a higher fraction of  $\alpha$ -Fe in the as-milled MA sample.

Figure 4 shows the hysteresis loops of MA and MM samples annealed within the temperature range of 823 to 1023 K. They both exhibited single-phase magnetic behavior; that is, no two-phase steps could be observed on the demagnetization curves. The main differences between MA and MM samples were that the remnant magnetization,  $M_r$ , and coercivity,  $H_c$ , for the MM powders were larger values than that for the MA powders.

The effect of heat treatment temperature on the remanence,  $M_r$ , and coercivity,  $H_c$ , of MM and MA powders is shown in Fig. 5. Both the MA and MM powders showed maximum values of  $M_r$  at 873 to 923 K and then decreased with increasing temperature, but the value of MM powder was always higher than that of MA powders in the whole annealing temperature range. The maximum values of  $M_r$  for MM and MA samples were 112 emu/g and 108 emu/g, respectively. Because of the increase of the grain size, the value of  $M_r$  decreased with the decreasing annealing temperature. In the MA samples, the values of  $H_c$  increased slowly with increasing annealing temperature and reached a maximum of 3.5 kOe at 1023 K. Higher values of  $H_c$  were exhibited by the annealed MM samples, and a maximum value of 4.2 kOe was measured at the annealing temperature of 973 k.

In two-phase composite permanent magnet materials, it is supposed (Ref 16, 17, 22) that effective exchange coupling requires a fine and uniform grain structure and grain size comparable with the exchange length of the soft phase  $L_{ex} = [A(J_c/\mu_0)^2]^{1/2}$  (Ref 16), or less than twice the width of the domain wall of the hard phase  $\delta = (A/K)^{1/2}$  (Ref 22), which is for  $\text{Nd}_2\text{Fe}_{14}\text{B}/\alpha\text{-Fe}$  nanocomposite magnets of  $\sim 10$  nm (Ref 22). ( $A$  is the exchange constant,  $J_s$  is the spontaneous magnetic polarization, and  $K$  is the anisotropy constant.) As noted, the average grain size of the MM material was smaller than that of the MA material. Hence, it is to be expected that exchange coupling would be more effective in the annealed MM powders which would account for the higher values of remanence and coercivity.

## 4. Conclusions

The structure and magnetic properties of MA and MM  $\text{Nd}_8\text{Fe}_{88}\text{B}_4$  were studied. Both MM and MA resulted in a mixture  $\alpha$ -Fe and an amorphous phase. After annealing at temperatures above 823 K, both MA and MM samples showed very similar phase compositions. However, the average grain size of annealed MA powders was larger than that of annealed MM powders. As a consequence, both the remnant magnetization and coercivity of annealed MM powders were superior to those of annealed MA powders.

## References

1. J.S. Benjamin, *Metall. Trans.*, Vol 1, 1970, p 2954
2. C.C. Koch, *Annu. Rev. Mat. Sci.*, Vol 15, 1989, p 121
3. L. Schultz, K. Schnitzke, J. Wecker, M. Katter, and C. Kuhrt, *J. Appl. Phys.*, Vol 70, 1991, p 6339

4. T. Harada and T. Kuji, *J. Appl. Phys.*, Vol 72, 1992, p 5443
5. Y.S. Cho and C.C. Koch, *J. Alloys Comp.*, Vol 61, 1987, p 3583
6. L. Schultz, J. Wecker, and E. Hellstern, *J. Appl. Phys.*, Vol 61, 1987, p 3583
7. T. Harada and T. Kuji, *J. Alloys Comp.*, 1996, Vol 232, 1996, p 238
8. G. Veitl, B. Scholz, and H.D. Kunze, *Mater. Sci. Eng. A*, Vol 134, 1991, p 1410
9. K. Sakurai, Y. Yamada, C.H. Lee, T. Fukunaga, and U. Mizutani, *Mater. Sci. Eng. A*, Vol 134, 1991, p 1414
10. A.R. Yavari and P.J. Desre, *Mater. Sci. Forum*, Vol 43, 1992, p 89-90
11. L. Schultz and J. Wecker, *Mater. Sci. Eng.*, Vol 99, 1988, p 127
12. W. Gong, G.C. Hadjipanayis, and R.F. Krause, *J. Appl. Phys.*, Vol 75, 1994, p 6649
13. J. Ding, P.G. McCormick, and R. Street, *J. Magn. Magn. Mater.*, Vol 1, 1993, p 124
14. R. Coehoorn, D.B. Mooij, and C.D.E. Waard, *J. Magn. Magn. Mater.*, Vol 80, 1989, p 101
15. A. Manaf, R.A. Buckley, H.A. Davies, and Leonowicz, *J. Magn. Magn. Mater.*, Vol 101, 1991, p 360
16. T. Schrefl, R. Fischer, J. Fidler, and H. Kronmuller, *J. Appl. Phys.*, Vol 76, 1994, p 7053
17. E.F. Kneller and R. Hawig, *IEEE Trans. Magn. MAG-27*, 1991, p 3588
18. L. Schultz et al., *Mater. Sci. Eng.*, Vol 97, 1988, p 127
19. R.M. Davis, B. McDermott, and C.C. Koch, *Metall. Trans. A*, Vol 19, 1988, p 2867
20. Ch. Kuhrt and L. Schultz, *J. Appl. Phys.*, Vol 71, 1992, p 1896
21. W.F. Miao, J. Ding, P.G. McCormick, and R. Street, *J. Appl. Phys.*, Vol 79, 1996, p 2079
22. J.M.D. Coey, *J. Magn. Magn. Mater.*, Vol 1041, 1995, p 140-144